01 Jan 2016

A Spatial-dynamical Framework For Evaluation Of Satellite Rainfall Products For Flood Prediction

Felipe Quintero

Witold F. Krajewski

Ricardo Mantilla

Scott Small

et. al. For a complete list of authors, see https://scholarsmine.mst.edu/civarc_enveng_facwork/2648

Recommended Citation

F. Quintero et al., "A Spatial-dynamical Framework For Evaluation Of Satellite Rainfall Products For Flood Prediction," *Journal of Hydrometeorology*, vol. 17, no. 8, pp. 2137 - 2154, American Meteorological Society, Jan 2016.

The definitive version is available at https://doi.org/10.1175/JHM-D-15-0195.1

A Spatial–Dynamical Framework for Evaluation of Satellite Rainfall Products for Flood Prediction

FELIPE QUINTERO, WITOLD F. KRAJEWSKI, RICARDO MANTILLA, SCOTT SMALL, AND BONG-CHUL SEO

Iowa Flood Center, The University of Iowa, Iowa City, Iowa

(Manuscript received 10 October 2015, in final form 19 May 2016)

ABSTRACT

Rainfall maps that are derived from satellite observations provide hydrologists with an unprecedented opportunity to forecast floods globally. However, the limitations of using these precipitation estimates with respect to producing reliable flood forecasts at multiple scales are not well understood. To address the scientific and practical question of applicability of space-based rainfall products for global flood forecasting, a data evaluation framework is developed that allows tracking the rainfall effects in space and time across scales in the river network. This provides insights on the effects of rainfall product resolution and uncertainty. Obtaining such insights is not possible when the hydrologic evaluation is based on discharge observations from single gauges. The proposed framework also explores the ability of hydrologic model structure to answer questions pertaining to the utility of space-based rainfall observations for flood forecasting. To illustrate the framework, hydrometeorological data collected during the Iowa Flood Studies (IFloodS) campaign in Iowa are used to perform a hydrologic simulation using two different rainfall–runoff model structures and three rainfall products, two of which are radar based [stage IV and Iowa Flood Center (IFC)] and one satellite based [TMPA–Research Version (RV)]. This allows for exploring the differences in rainfall estimates at several spatial and temporal scales and provides improved understanding of how these differences affect flood predictions at multiple basin scales. The framework allows for exploring the differences in peak flow estimation due to nonlinearities in the hydrologic model structure and determining how these differences behave with an increase in the upstream area through the drainage network. The framework provides an alternative evaluation of precipitation estimates, based on the diagnostics of hydrological model results.

1. Introduction

Global-scale flood forecasting systems are currently being developed, evaluated, and improved (Wu et al. 2014). These forecasting systems rely on two separate but equally important components: 1) global-scale, near-real-time precipitation estimates and 2) hydrological models that partition rainfall into runoff components and route runoff to predict streamflow fluctuations at various basin outlets.

Multiple papers in the literature over the past 30 years document efforts to address the first component of using satellite observations to estimate global precipitation. Recent summaries of these efforts are discussed by Kucera and Lapeta (2014), Qu and Powell (2013), Gebremichael and Hossain (2010), and Kidd and Levizzani (2010), among others. A common thread in the literature is the acknowledgment of considerable uncertainty associated with space-based precipitation estimates (Young et al. 2014; Maggioni et al. 2014; Gebregiorgis and Hossain 2014; Moazami et al. 2014). This uncertainty is well documented by the leading space agencies around the world as they continue to support ground validation efforts in which space-based precipitation estimates are evaluated by comparisons with reference estimates, which are typically based on data from weather radar and rain gauge networks. Ground validation studies show that, in general, uncertainty increases as the space–time resolution (scale) decreases (e.g., Lo Conti et al. 2014; Stampoulis and Anagnostou 2012).

The hydrological models that partition rainfall into runoff components and route runoff to predict

Corresponding author address: Felipe Quintero, Iowa Flood Center, The University of Iowa, Maxwell Stanley Hydraulics Lab 135, Iowa City, IA 52242.
E-mail: felipe-quintero@uiowa.edu

DOI: 10.1175/JHM-D-15-0195.1

streamflow fluctuations represent the second key component of global flood forecasting systems. These models are constructed to obey basin boundaries, which are defined by the selection of points of interest (e.g., major cities) along the river network. In a global system, all of the millions of possible basins should be represented, which poses a computational challenge. Current global-scale forecasting systems address this issue by selecting a minimum drainage area (subbasin) for which the runoff processes are represented (Wu et al. 2014).

This brief discussion addresses the issue of uncertainty across spatial and temporal scales of precipitation estimates and hydrologic rainfall–runoff models and leads us to formulate a question of scientific and practical significance: Given the limitations inherent in both space–time resolution and the accuracy of space-based precipitation estimates, what is the basin scale at which global flood forecasting models are useful? Our objective in this paper is to organize a data evaluation framework to address this question rather than answering the question. We use data gathered during the Iowa Flood Studies (IFloodS; Petersen and Krajewski 2013) to illustrate our framework and to draw preliminary conclusions.

Three requirements are necessary in order to use this framework for space-based data analysis. First, a well-instrumented study domain should be large enough to include a considerable range of spatial and temporal scales. Second, the investigated space-based precipitation estimates over a uniform period of time should be accompanied by ground-based reference precipitation estimates. Third, we need a distributed hydrological model that allows us to distinguish the effects of the input uncertainty from the model specific assumptions.

All of these requirements are satisfied within the confines of the IFloodS campaign. The study area is over 50 000 km^2, with the largest basins draining areas as large as 30 000 km^2. The second requirement is addressed by the fact that multiple space-based precipitation estimates are accompanied by high-quality multisensor reference rainfall mapping that is based on data from several weather radars and numerous in situ instruments (Petersen and Krajewski 2013). Finally, a flexible hydrological model developed by the Iowa Flood Center (IFC) has been implemented and evaluated for the region (e.g., Cunha et al. 2012; Seo et al. 2012; Ayalew et al. 2014). The model has the ability to estimate streamflow fluctuations for headwater basins as small as 0.1 km^2 and as large as the largest scales considered here, and it does not rely on calibrated parameters.

Our paper is organized as follows. In section 2, we review previous studies that use space-based precipitation estimates to force hydrologic models and, subsequently, to establish the need for a systematic data analysis framework relevant to flood prediction. In section 3, we describe our spatiodynamic data evaluation framework for space-based precipitation estimates. Section 4 describes data used in this study, and section 5 presents the results of the study using the IFloodS experiment dataset. Finally, we discuss the results with respect to the findings that arose when we used the proposed framework.

2. Review of flood forecasting using space-based precipitation estimates

During the past decade, multiple efforts have been made to forecast floods using space-based precipitation estimates (e.g., Bitew and Gebremichael 2011; Jiang et al. 2012; Tong et al. 2014; Casse et al. 2015; Li et al. 2015; Worqlul et al. 2015; Zhao et al. 2015; Chintalapudi et al. 2014; Knoche et al. 2014; Nikolopoulos et al. 2013; Maggioni et al. 2013; Vergara et al. 2014; Thiemig et al. 2013; Wu et al. 2012; Gourley et al. 2011; Behrangi et al. 2011; Nikolopoulos et al. 2010; Harris and Hossain 2008).

The literature identifies two major approaches used to address the propagation of space-based rainfall estimation error in hydrologic simulation. The first is a deterministic approach in which the space-based rainfall estimates are first compared against a reference and then examined with regard to the differences in the streamflow properties obtained from the space-based forcing and the reference (Chintalapudi et al. 2014; Thiemig et al. 2013; Serpetzoglou et al. 2010). The second approach is probabilistic and consists of first producing an ensemble of possible realizations of space-based rainfall derived from a statistical model and then forcing the hydrologic model with each member of the ensemble. The spreading of the hydrological simulations provides a quantification of the propagation of rainfall uncertainty to flow simulations (e.g., Demaria et al. 2014; Maggioni et al. 2013, 2011).

The reference commonly used to characterize uncertainties in space-based rainfall estimates is obtained from ground-based data, often from rain gauge data (e.g., Gebremichael and Krajewski 2004; Villarini and Krajewski 2007). However, although rain gauge networks provide reliable information about rainfall at the ground level, their sparseness often impedes the ability to characterize the spatial structure of the uncertainties. Another possibility consists of using a benchmark rainfall field that is derived from multiple instruments. Many authors have also compared different space-based rainfall products to rainfall estimates by combining weather radar and gauge data (Mehran and AghaKouchak 2014; Chintalapudi et al. 2014; Stampoulis et al. 2013; Nikolopoulos et al. 2013; Vergara et al. 2014; Habib et al.

2012; Gourley et al. 2011; Anagnostou et al. 2010). However, since radar rainfall is associated with significant uncertainties [see review by Villarini and Krajewski (2010)], comparing space-based rainfall with such references allows the analysis of only an approximate error structure at multiple scales and yields only a limited understanding of how these errors propagate with an increase in the drainage area of the basins. Hossain and Anagnostou (2006) pointed out that although these kinds of studies provide useful information about satellite rainfall uncertainties, many focus on the accumulation over large spatiotemporal scales and do not provide insight into the smaller scale that is more relevant to the flood processes.

Analysis of spatial (and temporal) resolution determines, to some degree, the feasible scales at which space-based rainfall can provide reliable hydrological simulations. Some authors have addressed the problem of determining how errors in hydrologic simulations are related to the scales in space-based rainfall (Nikolopoulos et al. 2010; Lee and Anagnostou 2004). However, there are still obstacles that get in the way of addressing our central question: What is the basin scale at which global flood forecasting models are useful? Wu et al. (2012) argue that global flood modeling systems are useful for predicting floods with durations of over a day or a few days but that they should not be expected to consistently detect shorter-term floods. However, their results lack an analysis of the relationship between relevant prediction errors and basin area. The consensus is that the performance of hydrologic simulation increases as a function of the area of the basin, and the spread of differences increases with a decrease in drainage area (e.g., Vergara et al. 2014; Nikolopoulos et al. 2013, 2010).

With respect to the effect of the complexity of the hydrologic model structure when forced with space-based rainfall products, Harris and Hossain (2008) used the Soil Conservation Service (SCS) curve number method, the Green–Ampt infiltration method, the deficit/constant loss method, and the TOPMODEL, which is forced with NASA 3B41RT rainfall (where RT stands for real time). In terms of minimizing flood prediction uncertainty, they found the SCS curve number method to be most effective, followed by the Green–Ampt infiltration and deficit/constant loss methods, but it is unclear if these conclusions hold universally. Other authors (e.g., Nikolopoulos et al. 2010) have shown the effect of the highly nonlinear rainfall–runoff transformation for assessing peak flows with different satellite products.

The above literature review reveals considerable interest in and effort devoted to the topic. However, we have found that there is much disagreement in terms of how useful it is to use space-based rainfall to forecast floods. Clearly, the satellite rainfall products have certain space–time resolutions (known) and time- and space-variable uncertainty structures (largely unknown). The resolution alone imposes some degree of limitation on the usefulness of the resulting hydrologic prediction (meant here for streamflow or flooding). Hydrologic models are also subject to structural and parametric uncertainty. Important questions that remain unanswered include how the two sources of uncertainty interact, if they cancel or amplify each other, and what is the role of the systematic versus random components of the uncertainty?

Based on the literature review, we attempted to determine which basin scales are adequate for the applications of space-based rainfall estimates. We analyzed the quality of the results obtained by different authors when performing streamflow simulations in basins of hundreds of square kilometers (Harris and Hossain 2008; Gourley et al. 2011; Nikolopoulos et al. 2013), thousands of square kilometers (Nikolopoulos et al. 2010; Behrangi et al. 2011; Maggioni et al. 2013; Vergara et al. 2014; Chintalapudi et al. 2014; Knoche et al. 2014; Worqlul et al. 2015; Zhao et al. 2015), hundreds of thousands of square kilometers (Wu et al. 2012; Thiemig et al. 2013; Casse et al. 2015), and millions of square kilometers (Li et al. 2015). Based on this ad hoc analysis, the conclusions are inconsistent. Using space-based rainfall for hydrology seems to be promising in some cases, especially at larger scales (Wu et al. 2012; Thiemig et al. 2013; Li et al. 2015), while it seems disappointing in other cases (Knoche et al. 2014; Worqlul et al. 2015). In some instances, satisfactory results seem to be achievable only by calibrating hydrologic models individually to rainfall products (Gourley et al. 2011; Nikolopoulos et al. 2013). We speculate that these inconsistencies arise, in part, because producing statements about the quality of the results of the hydrologic simulation is traditionally based on and limited to observing the consistency of the hydrographs that are derived from the model at particular points of interest in the drainage network.

As we will explicate later in the paper, many conclusions in the above studies are drawn based on a hydrograph comparison at the outlet of a basin, which makes the results susceptible to random occurrences in terms of the timing and location of errors in the satellite product, especially at smaller scales. Worse yet, while river basins can filter out small-scale (relatively speaking) uncertainties and rainfall variability (Ayalew et al. 2013), systematic errors at the outlet can be corrected by hydrologic model calibration. However, this calibration has several problems associated with it. Not only does it obscure our understanding of how the data/model combination really works, but in the context of worldwide applications of satellite data for flood prediction, it is also

simply infeasible in many parts of the planet. Therefore, our efforts should go toward creating systems that are robust and that are based on information that is readily available everywhere, which mainly includes topography and land use with the associated understanding of the runoff-generating mechanism.

The abovementioned discussion reveals the lack of a common framework from which to address the basin scale, satellite data resolution and uncertainty, and hydrologic model structure that is necessary in order to answer many questions regarding the usefulness of space-based rainfall observations for flood forecasting. Below, we propose a spatial–dynamic framework to address these issues.

3. Methodology

The development of a framework that helps us understand the benefits and limitations of space-based rainfall products in hydrological forecasting requires the design of several experiments that collectively provide meaningful insight into how the aspects of hydrographs that are relevant to the problem of flood forecasting change in space and time. The hydrologic context of examining the uncertainty of satellite rainfall products imposes a condition that a basin of interest is set. Generically, this implies that we desire the capacity to predict streamflow everywhere in the basin. Consequently, the space–time location of the errors is as important as the scale dependence of these errors. Simply put, knowledge that is limited to a description of how uncertainties depend on space–time scale, while important, is not sufficient to determine its effect on the hydrologic outcome because the river basin drainage network and its topological configuration affect water transport throughout the basin as well as the basin's ability to filter out random uncertainties across scales.

In this study, we depict this aspect both with and without a watershed context. Using the watershed context can be limited to rainfall-only considerations, or it could be extended to include the effects of water transport throughout the drainage network and rainfall–runoff transformation with or without considering the memory of the system. We will illustrate these conditions using hydrologic models with similar, though not identical, structures. To demonstrate the effect of delays in the effects of rainfall on streamflow, we use a (linear) model with a simple runoff generation mechanism and constant river velocity formulation. To explain the effects of system memory, we extend the model to include nonlinear components in runoff generation and water transport in the drainage network. Neither model is calibrated to fit the observed hydrograph at a particular outlet. In fact, this aspect is not highly relevant for the purpose of our illustration. Therefore, we will present a set of four analyses of satellite rainfall uncertainty: 1) scale dependency only, 2) scale dependency and watershed context, 3) transport effect across river basin, and 4) transport and memory effects across river basins.

These analyses share a fundamental requirement—a reference rainfall product. To avoid diverting the focus away from the main purpose of this paper, we do not discuss this aspect in detail. Suffice it to say that the best opportunity for a high-quality, ground-based rainfall product is a combination of a dense network of rain gauges (and/or disdrometers) and modern weather radars. While we do not argue for a specific radar-based product to be used as a reference, many current efforts around the globe are devoted to improving existing methods. In the context of satellite product validation, ground-based validation campaigns complement operational facilities and provide enhanced products (e.g., Delrieu et al. 2014; Kirstetter et al. 2014).

Use of our proposed framework also imposes certain conditions on the hydrologic model structure. The model should faithfully represent the drainage network and its function in transporting the water. There is a plethora of distributed hydrologic models with sufficiently high spatial resolution that are potentially available for this analysis, but our framework calls for a model that does not require calibration and that has a simple enough structure to reveal important aspects of rainfall input. The no-calibration requirement is a simple reflection of the fact that the calibration process compensates for the uncertainties in the rainfall input in addition to uncertainties that arise from other sources (Seo et al. 2012). Since our interest is in evaluating the hydrologic impact of the rainfall products, the hydrologic model should be as independent as possible of those products.

The models we use build on the concept of landscape decomposition into hillslopes and channels (Mantilla and Gupta 2005) and allow for flexible structure and the representation of the physical processes of runoff generation and water transport. The set of differential equations describing change in water storages and discharge are solved using a modern parallelized implementation of numerical Runge–Kutta methods (Small et al. 2013). We demonstrate how different model structures lead to different insights with respect to rainfall input. The use of hydrologic models extends the insights that can be obtained from considering rainfall-only discrepancies.

Diagrams in Figs. 1–3 provide a schematic representation that summarizes all of the considered aspects. In Fig. 1, we define a ''traditional'' framework of evaluating a given rainfall product against a reference product without a watershed context. For a given time

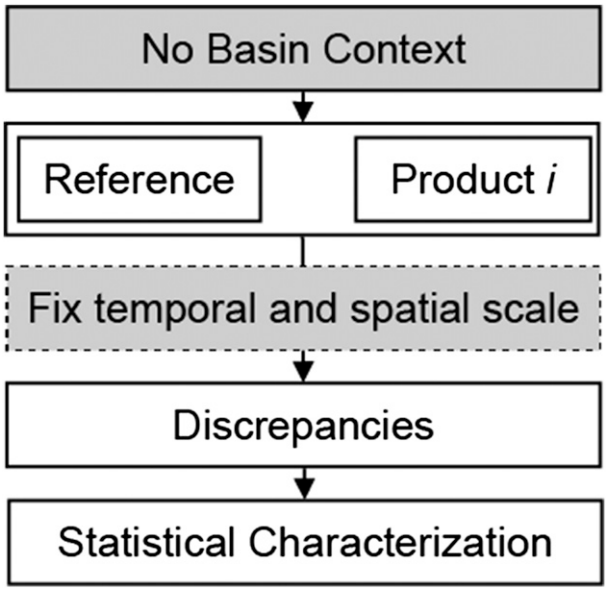

FIG. 1. Schematic representation of the traditional framework for the evaluation of rainfall products without consideration of the watershed context.

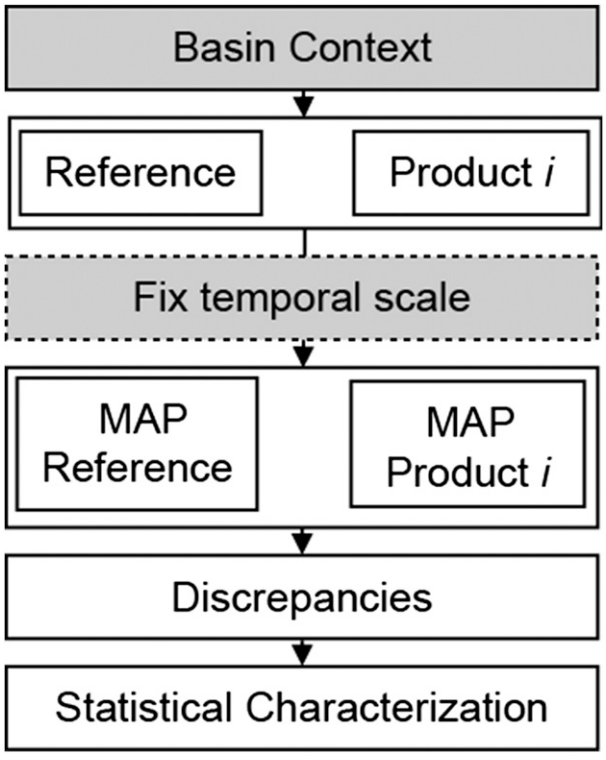

FIG. 2. Schematic representation of the framework for the evaluation of rainfall products with consideration of the watershed context through its mean areal precipitation (MAP).

scale of the products, one can calculate the spatial-scale dependency of the product discrepancy from the reference. We use the term ''discrepancy'' rather than ''error'' to emphasize that the reference is not the actual value (as the unfortunate but frequently used term ''ground truth'' implies). In Fig. 2, we introduce a watershed context and consider rainfall-only discrepancies. This requires integrating time-accumulated rainfall over each subbasin. This integration approach is analogous to the one shown in Cunha et al. (2015). We define the subbasins by the location of the stream segment junctions. Clearly, the smallest subbasins correspond to the outlets of first-order streams [see Rodríguez-Iturbe and Rinaldo (2001) for definitions] and the largest correspond to the outlet of the entire river basin. The time-accumulated rainfall of the product and its reference over each subbasin can be evaluated using a comparison metric, for example, percent normalized difference.

In Fig. 3, we introduce a hydrologic model for a transformation of the rainfall into runoff and streamflow. For example, one could compare peak flows calculated for each stream network segment. Since the small basins respond much faster than the large ones, the peak flow comparison must occur over a time window that is long enough to include responses at all scales. The longer the window, the greater the likelihood that another rainfall event may result in a peak that is larger than the original one, especially at small scales. This apparent complication can be easily resolved if the analysis is performed dynamically, that is, stepping through time with short steps. Also, depending on the type of hydrologic model used, one can observe the effects of the system memory or only the runoff translation. We return to this issue when discussing the specific results of the framework illustration.

To illustrate the framework, we use the data from the IFloodS ground validation campaign that transpired in eastern Iowa in the spring of 2013 (Petersen and Krajewski 2013). Although many ground- and space-based products have been available following the campaign, we use only a couple of radar-based products and one space-based product to illustrate the proposed framework. We leave the comprehensive study of the remaining products for future studies. Before we discuss the results, we will briefly describe the data and the models we used.

4. IFloodS data and models

a. Study area

The study area includes the river basins of the Turkey River, upstream of Garber, Iowa, and the Iowa River, upstream of Wapello, Iowa, that includes the Cedar River basin. We used six locations with available stream gauge data, shown in Fig. 4, as validation points. The land use in the basins is mainly agricultural, as the rich soils are used for growing corn and soybeans.

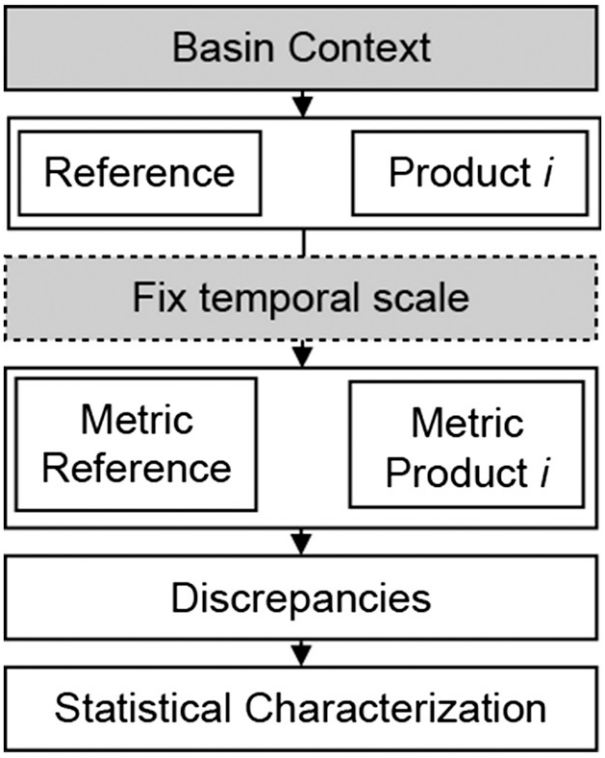

FIG. 3. Schematic representation of the framework for the evaluation of rainfall products using hydrologic models through the characterization of the discrepancies in hydrologic characteristics.

b. Rainfall datasets

The nominal period of the campaign was from 1 April to 30 June, and many instruments were deployed throughout this period. The main observational period was from 1 May through 15 June, the time when NASA's S-band polarimetric radar (NPOL) was deployed. Since the campaign took place before the launch of the GPM core satellite, only the premission products can be used.

1) MULTISENSOR PRECIPITATION ESTIMATES

Stage IV is a national rainfall product derived from the hourly multisensor (radar and rain gauges) precipitation estimates that are produced and distributed by the National Centers for Environmental Prediction. The rainfall estimates are obtained from combining mosaicked radar data and a variable bias field that is computed hourly from rain gauge amounts. The bias field is sampled on the Hydrologic Rainfall Analysis Project (HRAP) 4-km resolution grid (Reed and Maidment 1999) using a weighted interpolation scheme, and it is applied to the radar product so that the spatial variability of rainfall resolved by radars is preserved and the amounts of rainfall are calibrated to rain gauge accumulations.

2) RADAR-ONLY PRECIPITATION ESTIMATES

The IFC radar rainfall product is the NEXRAD composite of seven S-band weather radars covering the entire state of Iowa, but it does not yet include dual-polarization information. The rainfall estimates are available at 5-min time resolution and a spatial resolution of 0.004° cell size (~0.4 km). This product is the main forcing for the operational flood forecasting system implemented in the Iowa Flood Information System (IFIS; Demir and Krajewski 2013) and provides real-time flood warnings to all communities in Iowa. The radar product is not adjusted with information from rain gauges because of the lack of an adequate statewide automatic rain gauge network to perform this task and the time limitations inherent in operational systems.

3) SPACE-BASED PRECIPITATION ESTIMATES

The Tropical Rainfall Measuring Mission (TRMM) Multisatellite Precipitation Analysis (TMPA)–Research Version (TMPA-RV) was developed by NASA GSFC. The rainfall estimates are obtained using monthly calibration coefficients from microwave estimates that were previously calibrated (Huffman et al. 2010). The product is additionally calibrated monthly with ground reference data from the TRMM Combined Instrument (TCI) and Climate Anomaly and Monitoring System (CAMS). TMPA has a 3-h time resolution and a spatial resolution of 0.25° cell size (~28 km).

c. Discharge datasets

Stream gauge information is maintained by the USGS and provides river discharge data every 15 min. Figure 4 shows the location of the gauges. The significant discharges that occurred between 1 May and 15 June during the IFloodS period produced river stages that exceeded the moderate flood stage in the Turkey River at Garber (6.8 m with 605 $m^3 s^{-1}$) and the major flood stage in the Cedar River at Charles City (5.9 m with 583 $m^3 s^{-1}$), the Iowa River at Marengo (6.1 m with 1033 $m^3 s^{-1}$), and the Cedar River at Cedar Rapids (5.5 m with 1800 $m^3 s^{-1}$).

d. Hydrological model

1) LINEAR ROUTING AND CONSTANT RUNOFF MODEL

Figure 5a shows a representation of the model structure. We modeled three water storage components for every hillslope link: channel storage via a linear discharge relationship $q(t)$ ($m^3 s^{-1}$), water ponded on hillslope surface $s_p(t)$ (m), and effective water depth in hillslope subsurface $s_s(t)$ (m). The mass transport equation for each channel link in the network is given by

FIG. 4. Location of the six catchments considered in this study. The white circles at the outlets show the location of the USGS stream gauges. Brown circles show the location of the weather radars.

$$\frac{dq}{dt} = \frac{v_c}{l}\left[-q + (q_{\rm pc} + q_{\rm sc})\frac{A_h}{60} + q_{\rm in}(t)\right], \qquad (1)$$

where v_c is the channel flow velocity assumed to be constant in space and time, l is the channel link length, A_h is the area of the hillslope, $q_{\rm pc}$ is the flux that moves water from the water ponded on the surface to the channel and is defined by $q_{\rm pc} = k_2 s_p$, and $q_{\rm sc}$ is the flux that moves water from the subsurface to the channel and is defined by $q_{\rm sc} = k_3 s_s$. The function $q_{\rm in}(t)$ is the total discharge entering the channel from the upstream channels.

The mass conservation equations for surface and subsurface layers are given by

$$\frac{ds_p}{dt} = R_C p(t) - q_{\rm pc} - e_p \quad \text{and} \qquad (2)$$

$$\frac{ds_s}{dt} = (1 - R_C)p(t) - q_{\rm sc} - e_s, \qquad (3)$$

where R_C is the runoff coefficient and e_p and e_s are the surface and subsurface evapotranspiration and depend on the observed climatic actual evapotranspiration (see appendix A).

2) NONLINEAR ROUTING AND VARIABLE INFILTRATION MODEL

A representation of the model structure is shown in Fig. 5b. We modeled four water storage components for every hillslope link: channel storage via a linear discharge relationship $q(t)$ ($\rm m^3\,s^{-1}$), water ponded on hillslope surface $s_p(t)$ (m), effective water depth in the top soil layer $s_t(t)$ (m), and effective water depth in hillslope subsurface $s_s(t)$ (m). The mass transport equation for each channel link in the network is given by

$$\frac{dq}{dt} = \frac{v_r}{(1-\lambda_1)l}\left(\frac{q}{q_r}\right)^{\lambda_1}\left(\frac{A}{A_r}\right)^{\lambda_2} \times\left[-q + (q_{\rm pc} + q_{\rm sc})\frac{A_h}{60} + q_{\rm in}(t)\right], \qquad (4)$$

where λ_1 and λ_2 are exponents associated with the nonlinearity of flow velocity as a function of discharge and drainage area (see appendix B for more details on the transport equation). The mass conservation equations in the surface, top soil layer, and subsurface layers are given by

$$\frac{ds_p}{dt} = p(t) - q_{\rm pc} - q_{\rm pt} - e_p, \qquad (5)$$

$$\frac{ds_t}{dt} = q_{\rm pt} - q_{\rm ts} - e_t, \quad \text{and} \qquad (6)$$

$$\frac{ds_s}{dt} = q_{\rm ts} - q_{\rm sc} - e_s, \qquad (7)$$

where $q_{\rm pc}$ is the flux that moves water ponded on the surface to the channel and is defined by $q_{\rm pc} = k_2 s_p$, $q_{\rm pt}$ is

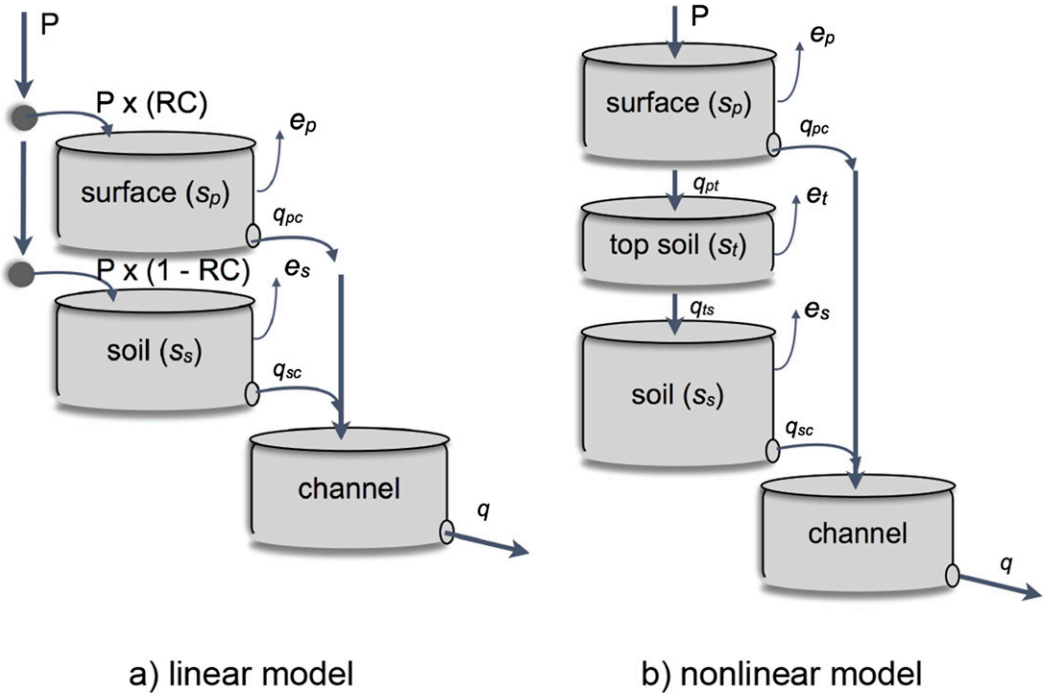

FIG. 5. Representation of the (a) linear and (b) nonlinear hydrologic models.

the flux that moves water ponded on the surface to the top layer storage and is defined by $q_{pt} = k_t s_p$, q_{ts} is the flux that moves water from the top layer storage to the subsurface is defined by $q_{ts} = k_i s_t$, and q_{sc} is the flux that moves water from the subsurface to the channel is defined by $q_{sc} = k_3 s_s$. The definitions of the terms k_2, k_t, k_i, and k_3 controlling the flux among storages, as well as the terms e_p, e_t, and e_s controlling evapotranspiration, are shown in appendix B.

To implement the models, we decomposed the landscape of the basins into hillslopes and channels derived from digital elevation maps at 90 m × 90 m cell size. We used these hillslopes as the hydrological response units where the runoff generation and transport processes occur. The average size of the hillslopes is approximately 0.4 km^2, which provides an accurate representation of the drainage network. Because of the large number of hillslopes in Iowa that were derived from this partitioning (~600 000), the resulting system of ordinary differential equations is large and required the development of a specialized numerical solver working in high-performance computers to provide a fast modeling solution (Small et al. 2013). Given the distributed structure of the hydrological models, we are able to produce discharge simulations at the outlet of every hillslope-link unit. Rainfall inputs are remapped to hillslope units using nearest neighbor interpolation. For the initial soil moisture conditions, we used values obtained through a spinup of the model with stage IV rainfall starting on 1 April, 4 weeks prior to the analyzed period.

5. Results

In this section, we illustrate the proposed framework using data from IFloodS. We limit our consideration to three products. We use stage IV data as a reference and compare them with one radar-only product (IFC rainfall) and one satellite-based product (TMPA). Other radar rainfall products were evaluated by Cunha et al. (2015) and Seo et al. (2015).

a. *Total rainfall accumulation without watershed context*

To illustrate the analysis concept presented in Fig. 1, we calculated maps of the rainfall accumulations of stage IV, IFC, and TMPA for the period between 1 May and 15 June at the study area. They are shown in Fig. 6. The two radar products show similar spatial patterns but differ in the magnitude of rainfall estimates, as can be expected by the different approaches used to produce the rainfall products, for example, stage IV is a radar rainfall gauge-corrected product while the IFC rainfall product is not. TMPA data exhibit a coarser spatial resolution but reveal a pattern similar to the one shown in the two radar products. This resolution is partially

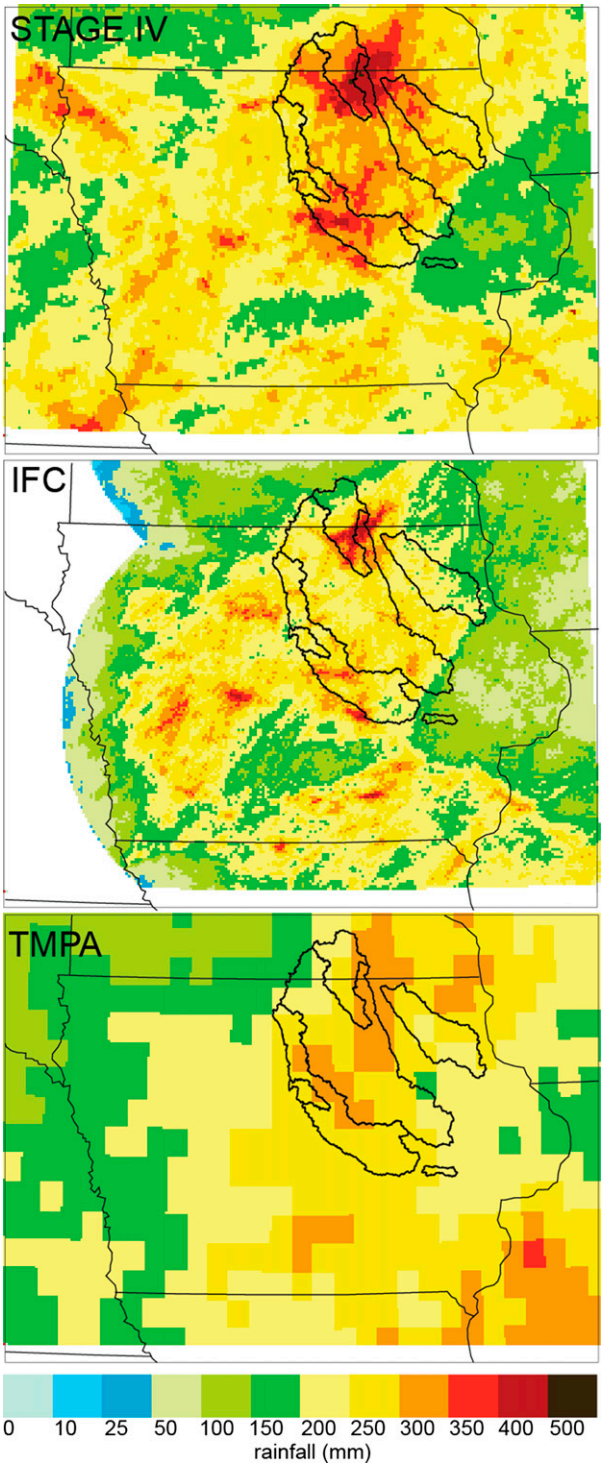

FIG. 6. Maps of accumulated rainfall over Iowa between 1 May and 15 Jun for stage IV, IFC, and TMPA.

responsible for the reduced range of the estimated total rainfall. It seems that the highest rainfall areas (e.g., in northern Iowa) are underestimated, while the lowest (e.g., in eastern Iowa) are overestimated relative to stage IV totals. At this spatial and temporal scale of analysis, the discrepancies reveal certain aspects related to the quality of the rainfall products, but they are insufficient in terms of explaining the effects of those discrepancies in the outputs of the hydrologic simulations (e.g., peak flow estimation).

Similarly, a plot of the differences in hourly rainfall compared to stage IV as a function of spatial scale (Fig. 7) reveals the uncertainty structure of radar rainfall (e.g., Seo and Krajewski 2010) and space-based rainfall with respect to six spatial scales (1, 2, 4, 8, 16, and 32 km). The uncertainty of radar rainfall shows greater discrepancies at higher spatial resolutions (1 km) than those at lower resolutions (32 km). A similar structure is observed for the space-based product, whereas for this case the discrepancies are larger than those for radar. These results may have implications for error propagation through distributed hydrologic models, especially for the problem of flood estimation at small basin scales. In the next section, we provide more information about these discrepancies across scales and consider the drainage network's filtering effect.

b. *Discrepancies in rainfall products at the subbasin scale*

To illustrate the analysis concept presented in Fig. 2, we calculated rainfall accumulation maps by adding hourly accumulations during the event between 24 May and 3 June and by spatially integrating the accumulations on every subbasin through the path of the flow in the drainage network. This sum adds up all the water that can flow through a particular link in the network. The dynamical capability of the framework allows us to select any temporal window to analyze the rainfall products. We selected these dates because severe thunderstorms and heavy rainfall during that event triggered the observed peak flows in the basins. Figure 8 shows the rainfall accumulation of the stage IV, IFC, and TMPA over the selected event. Figure 9 shows the accumulation differences of IFC and TMPA with the accumulations of stage IV. One can see that the larger discrepancies are found in the small-order channels and are more frequent on the satellite product. As a consequence of the spatial and temporal averaging of differences, discrepancies are reduced with the increment of drainage area. This type of map also reveals that localized discrepancies between rainfall products (e.g., the intense rainfall spot in central Iowa visible in stage IV but not present in the IFC product) propagate along the network, impacting the total volume of water that flows through flow-connected locations in the network.

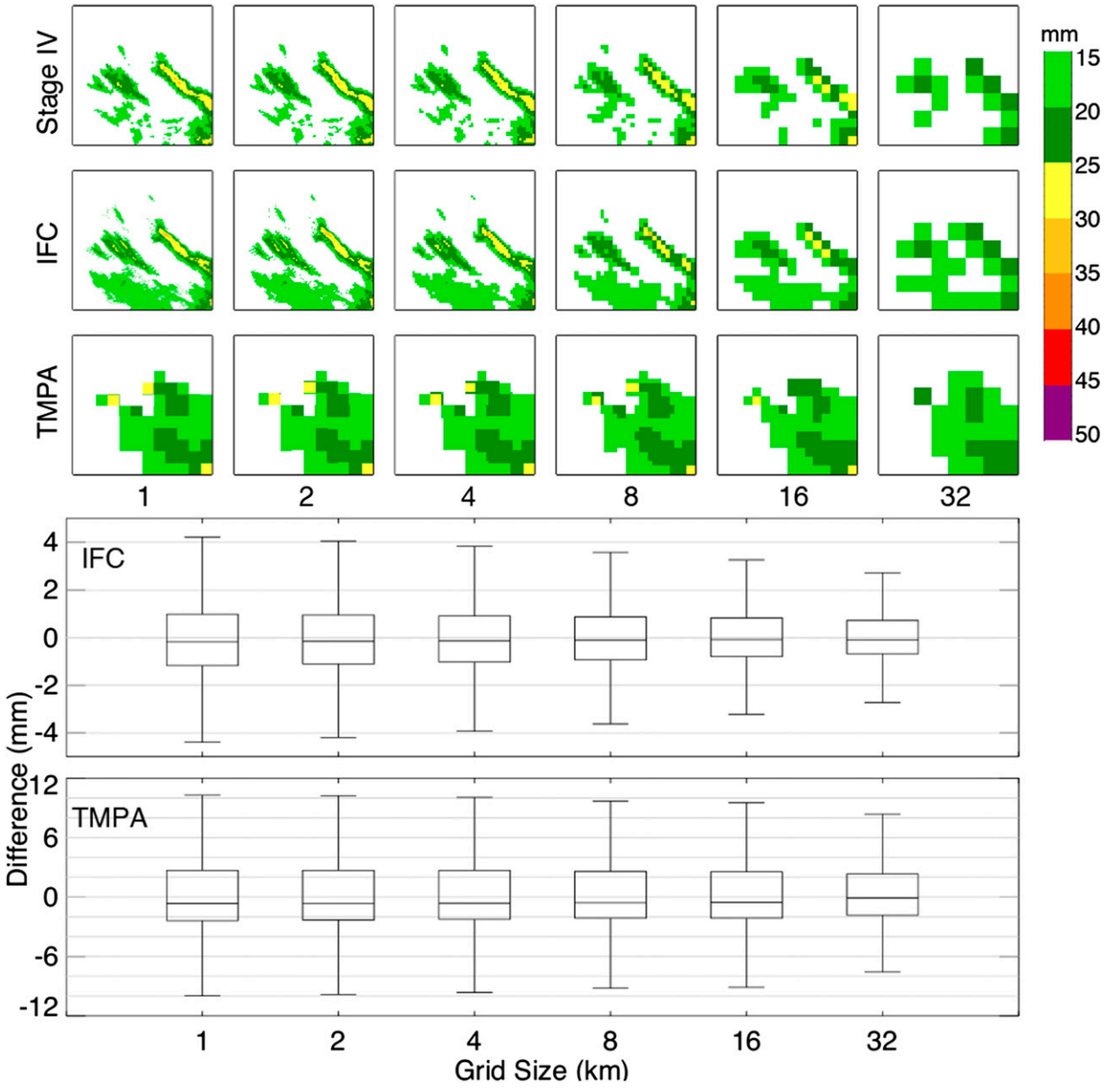

FIG. 7. (top) Hourly rainfall fields averaged spatially to different pixel sizes over a rectangular area containing to the six basins. (bottom) Scale-dependent structure of the differences between spatially averaged hourly rainfall fields (IFC and TMPA) and reference (stage IV).

c. *Sensitivity of hydrological simulations to rainfall input*

We forced the linear and nonlinear models with stage IV data in order to obtain the reference hydrographs that can be compared with hydrographs derived with other rainfall products. Figure 10 shows the results in the Cedar River basin at Charles City with the linear and nonlinear models. The simplicity of the linear model structure (red dotted line) makes it difficult to fit to the observed streamflow time series (black solid line), whereas the nonlinear model (red solid line) fits reasonably well to observations. Note that the parameter values for the nonlinear model are the same for all hillslopes and have been chosen to provide a reasonable performance across geographical settings and basin scales. The results we present in this section are influenced by the selection of parameters. However, the conclusions regarding the influence of model structure are generic and independent of this choice.

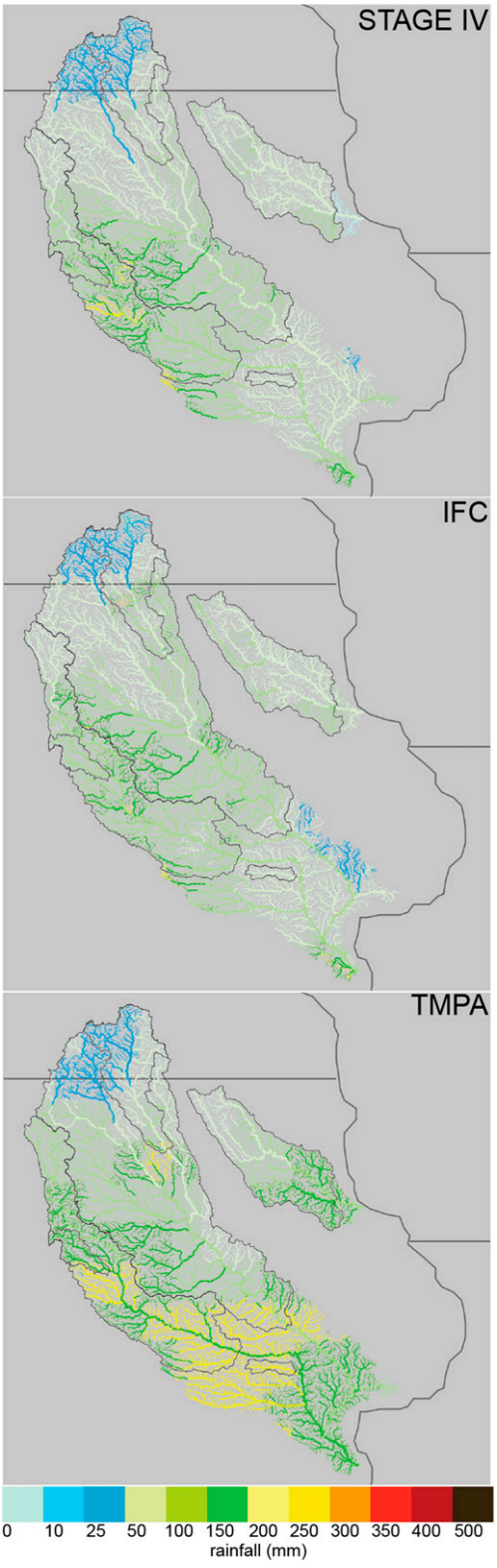

FIG. 8. Rainfall accumulation at the subbasin scale between 24 May and 3 Jun.

1) HYDROGRAPHS AT SELECTED BASINS

Figure 11 shows the hydrographs obtained at the selected basins when forcing the nonlinear model with radar and satellite rainfall products. The plots are sorted from smaller to larger drainage areas. In these plots we only show the hydrographs of the nonlinear model because the linear model produces too many flow fluctuations associated with every rainfall burst because of the simplicity of its structure. When comparing peak flows to the reference peak, the differences are larger in the catchments with smaller areas, especially for the satellite-based product. The results obtained in the larger basins seem to be satisfactory, with good agreement to the reference in both the radar- and satellite-derived hydrographs. These results show some evidence of inadequacy in terms of using satellite precipitation to produce an acceptable estimation of peak flow in catchments of small scales, which is caused by their coarser spatial resolution or satellite products compared to radar resolution. However, one would need to see the behavior of the simulations at every channel of the drainage network in order to gain a better understanding of this dependence of errors with drainage area and how they behave spatially.

2) ANALYSIS OF THE PROPAGATION OF ERRORS ALONG THE DRAINAGE NETWORK

We reduced the temporal scale to the event between 24 May and 3 June and extended the analysis to the entire drainage network instead of just selected basins. We use the framework to evaluate the discrepancies of hydrologic simulations at these scales.

We estimated the relative difference in the peak flow produced with the rainfall products compared to the peak produced by stage IV. Figure 12a shows the differences obtained with the linear model. This figure demonstrates that the larger differences in peak flows appear in the first-order streams of the drainage network and shows how the differences tend to be smaller as long as the peak propagates through the rivers. As drainage area increases, there is a trade-off caused by the spatial averaging between the overestimated (reddish) and underestimated (bluish) peak flows, which is compensated for downstream by producing smaller differences (white). Another visible aspect in the figure is how the discrepancies in a product with a coarser spatial resolution, like TMPA, affect much larger areas and a larger number of hillslopes. The locations of the differences in the drainage network are, consequently, related to the location of the storms in the rainfall products.

In Fig. 12b, we applied the same methodology but this time with the nonlinear model. The figure shows

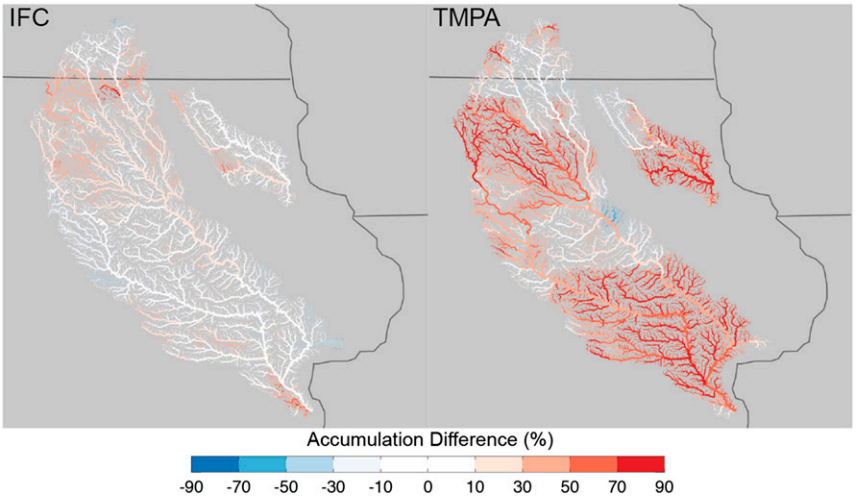

FIG. 9. Differences in rainfall accumulation at the subbasin scale compared to stage IV between 24 May and 3 Jun.

discrepancies of IFC and TMPA along the drainage network as previously explained in Fig. 12a. One can see that, despite using exactly the same rainfall products as in the linear case, other differences appear in the picture, which can be attributed to the nonlinear nature of the hydrological model. It means that, apart from the differences in the peak caused by the discrepancies in the rainfall products, the nonlinear model incorporates other differences into the system that are related to the model structure. It is necessary to keep in mind that the state variables in the nonlinear model are affected also by the discrepancies in the rainfall products that occur in the past (e.g., a previous event), and not only by the present rainfall, as happens with the linear model case. The linear model has short memory and forgets the discrepancies of rainfall products in the past, while in the nonlinear model those discrepancies remain tied to states of the model structure (i.e., soil moisture of the top layer). Using only a nonlinear model without comparing to a reference constructed with a linear model could lead to producing wrong statements about the differences in peaks that are not attributable completely to the rainfall products. One could make a similar statement with regard to the parameter values in the nonlinear model. A sensitivity analysis of parameter values can be performed to understand the role that different runoff mechanisms and routing velocities play in the overall propagation of discrepancies.

In Fig. 13 we show the portion of the hydrographs obtained during the selected event with the nonlinear model. We choose four points with and without available observed discharges in order to illustrate that depending on the selected location and the time

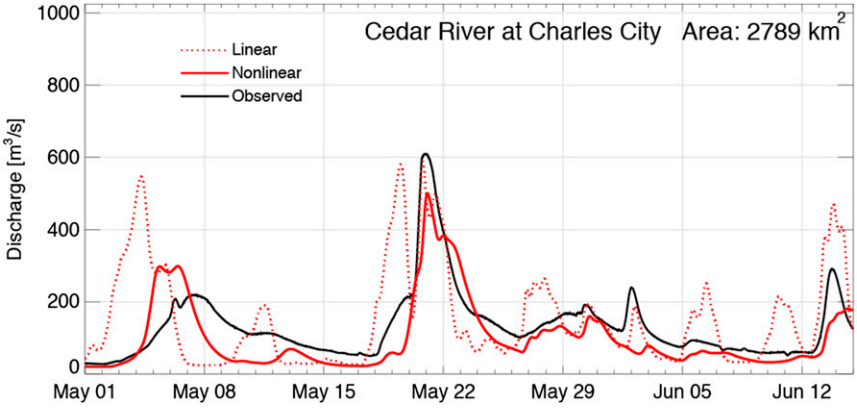

FIG. 10. Hydrographs produced using stage IV as forcing, with the linear (red dotted) and the nonlinear (red solid) model structures compared to observed discharge (black solid).

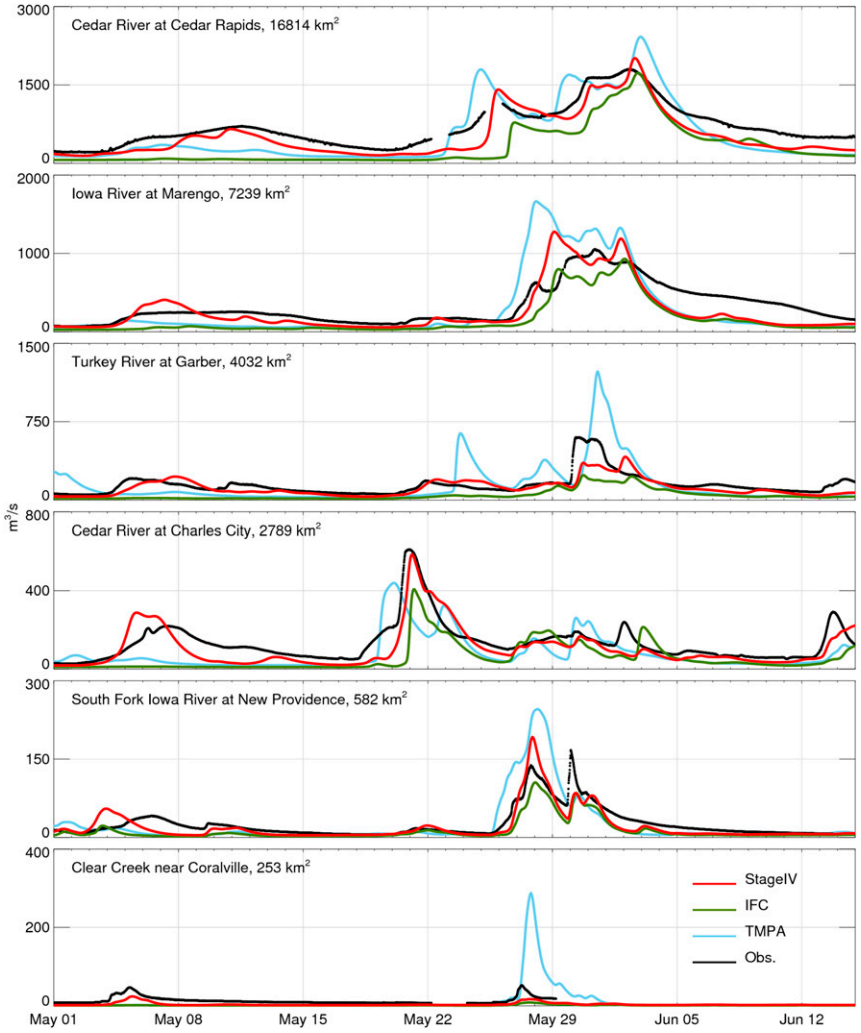

FIG. 11. The red line is the reference hydrograph produced with stage IV. The other hydrographs are derived from radar and satellite rainfall products. The black line shows the observed discharge.

period, the discrepancies shown in the hydrographs could be low, as in the case of Cedar River at Cedar Rapids, or contain large over- or underestimation, as is shown in the remaining three cases. Therefore, we consider that it is not reliable producing statements about the quality of rainfall products for hydrologic modeling based on site-specific comparison of time series, whereas the proposed framework approach provides a more complete description of the spatial and temporal behavior of the discrepancies that could be produced.

Figure 14 shows an example of the relationship between upstream area and the differences in peak flows at the selected event, between IFC and TMPA compared to the peaks of the reference provided by stage IV and the nonlinear model. The results illustrate how the errors propagate across spatial scales for different products at all the channels of the river network. The results are related to the effects of rainfall product resolution and uncertainty. To provide an adequate characterization of the errors in peak flow estimation from space-based products, the entire spectrum of spatial scales needs to be explored, not limited by the locations where discharge observations are available (shown in Fig. 14 as black dots). Such characterization requires subsequent statistical analyses that can be derived from the results of the framework, but that are outside of the scope of this paper [relevant issues are discussed in Mandapaka et al. (2009)]. It requires also doing considerations on the reliability of the hydrologic model and the rainfall product that are used as reference for benchmarking the comparisons.

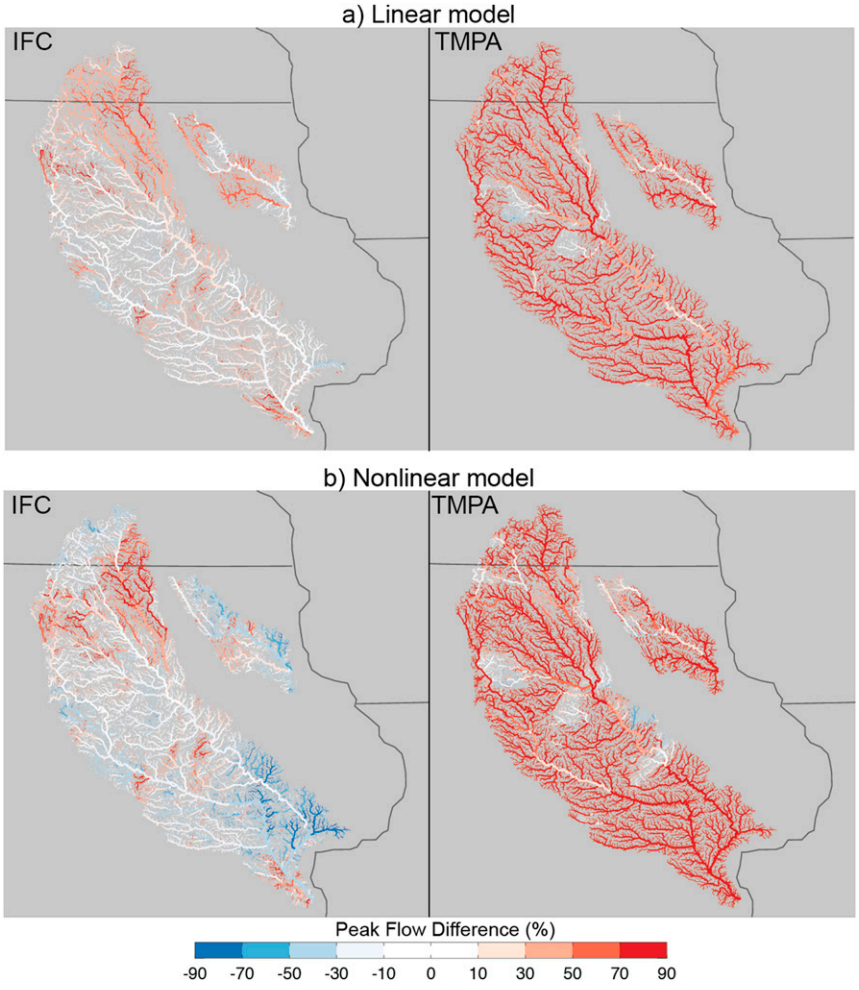

FIG. 12. Difference in peak flows obtained with the (a) linear and (b) nonlinear model structures.

6. Conclusions and recommendations

In this paper we introduced a concept of spatiodynamic framework for evaluating space-based precipitation estimates and their usefulness for flood forecasting. The framework provides tools for addressing the question of how the skill of flood forecasting driven by space-based rainfall products is distributed across spatial scales. Rather than evaluating particular space-based products from this perspective, we merely illustrated the framework and its advantages with a case study based on data collected in 2013 in Iowa during the IFloodS field campaign. We have been working on an operational implementation of this framework over the state of Iowa and will report the results in the near future. Here we just note that the framework is not designed specifically to evaluate space-based rainfall products. It can be used as easily to analyze any rainfall products, but those based on remote sensing products, that is, satellite or radar based, in particular.

Our analysis approach includes hydrologically relevant metrics for assessing the rainfall products. These metrics take into account the spatial and temporal aspects of the dynamics of the hydrologic response across scales using linear and nonlinear models. The framework provides an alternative evaluation of precipitation estimates that is based on the diagnostics of hydrological model results. The analysis framework can be extended to include other rainfall products and can use additional metrics of evaluation that reveal the rainfall effective scale of applicability for flood forecasting.

Based on our analysis, we conclude the following:

1) The scales where the hydrologic models suggest acceptable results in flood forecasting are not only related to the characteristics of the rainfall

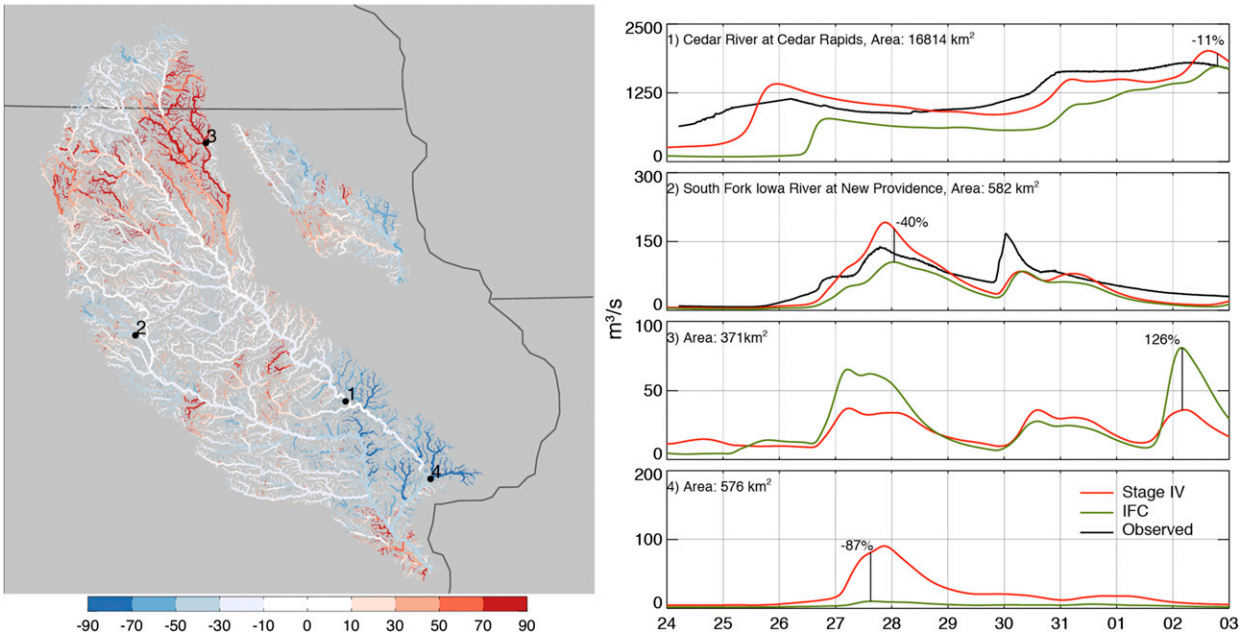

FIG. 13. Discrepancies in peak flows of the hydrographs obtained at four different locations over the drainage network with the IFC rainfall and the nonlinear model.

products, but also to the linearity/nonlinearity of the model structure that is used to make the evaluation. Our linear model structure with constant velocity exaggerated the occurrence of peaks in the hydrologic simulations and led to discrepancies with observed streamflow. However, the discrepancies in peak flows between simulations obtained with the linear model account only for differences in the rainfall inputs. This makes interpretation convenient and simple. When using a nonlinear model structure with variable flow velocity, these discrepancies in peaks account not only for differences in rainfall, but also to the effect of the memory of the system, that is, water stored in the soil and the drainage network.

2) Our framework highlights the relationship between the hydrologic prediction errors and the basin drainage area. The results we obtained are in agreement with the current consensus that performance of the hydrologic simulations improves as a function of the area of the basin and that the variance of the spread of the differences increases with the decrease in the drainage area (e.g., Vergara et al. 2014; Nikolopoulos et al. 2013, 2010). We illustrated the behavior of the discrepancies with drainage area at all scales of the subbasins of the network.
3) It is clear from our results that the topology of the river network plays an important role in averaging our errors in the rainfall inputs. We also demonstrated that this is not sufficient to eliminate errors in streamflow prediction at large scales. What also matters is the overall water amount fallen (estimated) over the basin and how this water travels to the outlet. The slowing of the water transport through subsurface flow and the threshold effects due to filled soil storage can substantially affect the resulting hydrographs. Calibration of hydrologic models masks these effects and thus we do not recommend performing it in rainfall input evaluation studies.

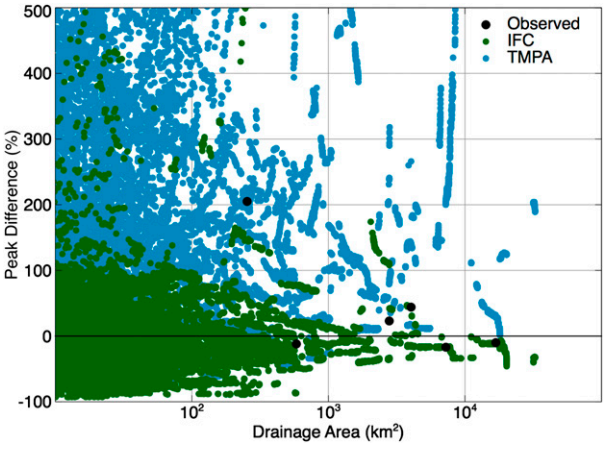

FIG. 14. Differences in peak flow across multiple scales between IFC and TMPA compared to stage IV using the nonlinear model. Includes the peak differences from gauges with discharge observations.

To the best of our knowledge, the insights that the spatiodynamic framework provides are missing in the literature. We hope that the capabilities offered by the framework will be helpful to the rainfall remote sensing community in the future studies motivated by hydrologic applications.

Acknowledgments. Funding for this work was provided by NASA Grants NNX13AD83G and NNX13AG94G (received by Witold Krajewski and Bong-Chul Seo), the Iowa Flood Center (received by Felipe Quintero, Ricardo Mantilla, and Scott Small), and National Science Foundation Award 1327830 (received by Witold Krajewski). We also gratefully acknowledge funding and management support from the NASA GPM and Precipitation Measurement Mission Programs for the Iowa Flood Studies field campaign. The authors thank all IFloodS participants for their effort to make the campaign successful.

APPENDIX A

Linear Model Equations

The parameters controlling the flux among storages are given by

$$k_2 = v_h \frac{L}{A_h} 60 \times 10^{-3} \ (\text{min}^{-1}) \quad \text{and} \tag{A1}$$

$$k_3 = v_g \frac{L}{A_h} 60 \times 10^{-3} \ (\text{min}^{-1}), \tag{A2}$$

where L and A_h are the length and area of the hillslope. Fluxes representing evaporation are given by

$$e_p = \text{corr}_{\text{evap}} c_p [e(t)] u \ (\text{m min}^{-1}), \tag{A3}$$

$$e_s = \text{corr}_{\text{evap}} c_s [e(t)] u \ (\text{m min}^{-1}), \tag{A4}$$

$$\text{corr}_{\text{evap}} = \begin{cases} \dfrac{1}{c_p + c_s}, & \text{if} \quad c_p + c_s > 1 \\ 1 & \text{otherwise} \end{cases}, \tag{A5}$$

$$c_p = \frac{s_p}{e(t)}, \tag{A6}$$

$$c_s = \frac{s_s}{e(t)}, \quad \text{and} \tag{A7}$$

$$k_i = k_2 \beta. \tag{A8}$$

The actual evapotranspiration function $e(t)$ depends on monthly climatological data. The runoff coefficient R_C is set equal to 0.5(0.001/60) for unit consistency, channel velocity $v_c = 0.75\,\text{m s}^{-1}$, velocity of water over the hillslope $v_h = 0.1\,\text{m s}^{-1}$, and velocity of water in the subsurface $v_g = 2.3 \times 10^{-5}\,\text{m s}^{-1}$. Note that variables c_s, c_p, k_i, and $\text{corr}_{\text{evap}}$ are intermediate calculations without physical definitions.

APPENDIX B

Nonlinear Model Equations

The parameters controlling the flux among storages are given by

$$k_2 = v_h \frac{L}{A_h} 60 \times 10^{-3} \ (\text{min}^{-1}), \tag{B1}$$

$$k_3 = v_g \frac{L}{A_h} 60 \times 10^{-3} \ (\text{min}^{-1}), \tag{B2}$$

$$k_i = k_2 \beta (\text{min}^{-1}), \quad \text{and} \tag{B3}$$

$$k_t = k_2 \left[A + B \left(1 - \frac{s_t}{S_L} \right)^{\alpha} \right] (\text{min}^{-1}). \tag{B4}$$

Fluxes representing evaporation are given by

$$e_p = \frac{\frac{s_p}{s_r} [e_{\text{pot}}(t)] u}{\text{corr}} \ (\text{m min}^{-1}), \tag{B5}$$

$$e_t = \frac{\frac{s_t}{s_L} [e_{\text{pot}}(t)] u}{\text{corr}} \ (\text{m min}^{-1}), \tag{B6}$$

$$e_s = \frac{\frac{s_s}{h_b - s_L} e_{\text{pot}}(t) u}{\text{corr}} \ (\text{m min}^{-1}), \quad \text{and} \tag{B7}$$

$$\text{corr} = \frac{s_s}{s_r} + \frac{s_t}{s_L} + \frac{s_s}{h_b - s_L}. \tag{B8}$$

Some parameters above are constant in time and take the same value at every channel. These are the channel reference velocity $v_r = 0.3\,\text{m s}^{-1}$, the exponent of channel velocity discharge $\lambda_1 = 0.3$ (dimensionless), the exponent of channel velocity area $\lambda_2 = -0.1$ (dimensionless), reference area $A_r = 1\,\text{km}^2$, reference discharge $q_r = 1\,\text{m}^3\,\text{s}^{-1}$, s_t is as previously defined in Eq. (4), e_{pot} is the potential evaporation, the velocity of water on the hillslope $v_h = 0.02\,\text{m s}^{-1}$, the infiltration from subsurface to channel $k_3 = 2.3 \times 10^{-5}\,\text{min}^{-1}$, the percentage of infiltration from top soil to subsurface $\beta = 0.005$ (dimensionless), the total hillslope depth $h_b = 0.5\,\text{m}$, the total topsoil depth $S_L = 0.1\,\text{m}$, the surface to topsoil infiltration additive factor $A = 0$ (dimensionless), the surface to topsoil infiltration multiplicative factor $B = 99$ (dimensionless), and the surface to topsoil infiltration exponent factor $\alpha = 3.0$ (dimensionless).

REFERENCES

Anagnostou, E. N., V. Maggioni, E. I. Nikolopoulos, T. Meskele, F. Hossain, and A. Papadopoulos, 2010: Benchmarking high-resolution global satellite rainfall products to radar and rain-gauge rainfall estimates. *IEEE Trans. Geosci. Remote Sens.*, **48**, 1667–1683, doi:10.1109/TGRS.2009.2034736.

Ayalew, T. B., W. F. Krajewski, and R. Mantilla, 2013: Exploring the effect of reservoir storage on peak discharge frequency. *J. Hydrol. Eng.*, **18**, 1697–1708, doi:10.1061/(ASCE)HE.1943-5584.0000721.

——, ——, ——, and S. J. Small, 2014: Exploring the effects of hillslope–channel link dynamics and excess rainfall properties on the scaling structure of peak-discharge. *Adv. Water Resour.*, **64**, 9–20, doi:10.1016/j.advwatres.2013.11.010.

Behrangi, A., B. Khakbaz, T. C. Jaw, A. AghaKouchak, K. Hsu, and S. Sorooshian, 2011: Hydrologic evaluation of satellite precipitation products over a mid-size basin. *J. Hydrol.*, **397**, 225–237, doi:10.1016/j.jhydrol.2010.11.043.

Bitew, M. M., and M. Gebremichael, 2011: Evaluation of satellite rainfall products through hydrologic simulation in a fully distributed hydrologic model. *Water Resour. Res.*, **47**, 1–11, doi:10.1029/2010WR009917.

Casse, C., M. Gosset, C. Peugeot, V. Pedinotti, A. Boone, B. Tanimoun, and B. Decharme, 2015: Potential of satellite rainfall products to predict Niger River flood events in Niamey. *Atmos. Res.*, **163**, 162–176, doi:10.1016/j.atmosres.2015.01.010.

Chintalapudi, S., H. Sharif, and H. Xie, 2014: Sensitivity of distributed hydrologic simulations to ground and satellite based rainfall products. *Water*, **6**, 1221–1245, doi:10.3390/w6051221.

Cunha, L. K., P. V. Mandapaka, W. F. Krajewski, R. Mantilla, and A. A. Bradley, 2012: Impact of radar-rainfall error structure on estimated flood magnitude across scales: An investigation based on a parsimonious distributed hydrological model. *Water Resour. Res.*, **48**, W10515, doi:10.1029/2012WR012138.

——, J. A. Smith, W. F. Krajewski, M. L. Baeck, and B.-C. Seo, 2015: NEXRAD NWS polarimetric precipitation product evaluation for IFloodS. *J. Hydrometeor.*, **16**, 1676–1699, doi:10.1175/JHM-D-14-0148.1.

Delrieu, G., L. Bonnifait, P.-E. Kirstetter, and B. Boudevillain, 2014: Dependence of radar quantitative precipitation estimation error on the rain intensity in the Cévennes region, France. *Hydrol. Sci. J.*, **59**, 1308–1319, doi:10.1080/02626667.2013.827337.

Demaria, E. M. C., B. Nijssen, J. B. Valdés, D. A. Rodriguez, and F. Su, 2014: Satellite precipitation in southeastern South America: How do sampling errors impact high flow simulations? *Int. J. River Basin Manage.*, **12**, 1–13, doi:10.1080/15715124.2013.865637.

Demir, I., and W. F. Krajewski, 2013: Towards an integrated Flood Information System: Centralized data access, analysis, and visualization. *Environ. Modell. Software*, **50**, 77–84, doi:10.1016/j.envsoft.2013.08.009.

Gebregiorgis, A. S., and F. Hossain, 2014: Estimation of satellite rainfall error variance using readily available geophysical features. *IEEE Trans. Geosci. Remote Sens.*, **52**, 288–304, doi:10.1109/TGRS.2013.2238636.

Gebremichael, M., and W. F. Krajewski, 2004: Assessment of the statistical characterization of small-scale rainfall variability from radar: Analysis of TRMM ground validation datasets. *J. Appl. Meteor.*, **43**, 1180–1199, doi:10.1175/1520-0450(2004)043<1180:AOTSCO>2.0.CO;2.

——, and F. Hossain, Eds., 2010: *Satellite Rainfall Applications for Surface Hydrology*. Springer, 327 pp.

Gourley, J. J., Y. Hong, Z. L. Flamig, J. Wang, H. Vergara, and E. N. Anagnostou, 2011: Hydrologic evaluation of rainfall estimates from radar, satellite, gauge, and combinations on Ft. Cobb basin, Oklahoma. *J. Hydrometeor.*, **12**, 973–988, doi:10.1175/2011JHM1287.1.

Habib, E., A. T. Haile, Y. Tian, and R. J. Joyce, 2012: Evaluation of the high-resolution CMORPH satellite rainfall product using dense rain gauge observations and radar-based estimates. *J. Hydrometeor.*, **13**, 1784–1798, doi:10.1175/JHM-D-12-017.1.

Harris, A., and F. Hossain, 2008: Investigating the optimal configuration of conceptual hydrologic models for satellite-rainfall-based flood prediction. *IEEE Geosci. Remote Sens. Lett.*, **5**, 532–536, doi:10.1109/LGRS.2008.922551.

Hossain, F., and E. N. Anagnostou, 2006: Assessment of a multidimensional satellite rainfall error model for ensemble generation of satellite rainfall data. *IEEE Geosci. Remote Sens. Lett.*, **3**, 419–423, doi:10.1109/LGRS.2006.873686.

Huffman, G. J., R. F. Adler, D. T. Bolvin, and E. J. Nelkin, 2010: The TRMM Multi-Satellite Precipitation Analysis (TMPA). *Satellite Rainfall Applications for Surface Hydrology*, M. Gebremichael and F. Hossain, Eds., Springer, 3–22, doi:10.1007/978-90-481-2915-7_1.

Jiang, S., L. Ren, Y. Hong, B. Yong, X. Yang, F. Yuan, and M. Ma, 2012: Comprehensive evaluation of multi-satellite precipitation products with a dense rain gauge network and optimally merging their simulated hydrological flows using the Bayesian model averaging method. *J. Hydrol.*, **452–453**, 213–225, doi:10.1016/j.jhydrol.2012.05.055.

Kidd, C., and V. Levizzani, 2010: Status of satellite precipitation retrievals. *Hydrol. Earth Syst. Sci. Discuss.*, **7**, 8157–8177, doi:10.5194/hessd-7-8157-2010.

Kirstetter, P.-E., Y. Hong, J. J. Gourley, Q. Cao, M. Schwaller, and W. Petersen, 2014: Research framework to bridge from the Global Precipitation Measurement Mission core satellite to the constellation sensors using ground-radar-based national mosaic QPE. *Remote Sensing of the Terrestrial Water Cycle*, V. Lakshmi et al., Eds., Wiley, 61–79, doi:10.1002/9781118872086.ch4.

Knoche, M., C. Fischer, E. Pohl, P. Krause, and R. Merz, 2014: Combined uncertainty of hydrological model complexity and satellite-based forcing data evaluated in two data-scarce semi-arid catchments in Ethiopia. *J. Hydrol.*, **519**, 2049–2066, doi:10.1016/j.jhydrol.2014.10.003.

Kucera, P., and B. Lapeta, 2014: Leading efforts to improve global quantitative precipitation estimation. *Bull. Amer. Meteor. Soc.*, **95**, ES26–ES29, doi:10.1175/BAMS-D-13-00078.1.

Lee, K.-H., and E. N. Anagnostou, 2004: Investigation of the nonlinear hydrologic response to precipitation forcing in physically based land surface modeling. *Can. J. Rem. Sens.*, **30**, 706–716, doi:10.5589/m04-037.

Li, Z., D. Yang, B. Gao, Y. Jiao, Y. Hong, and T. Xu, 2015: Multiscale hydrologic applications of the latest satellite precipitation products in the Yangtze River basin using a distributed hydrologic model. *J. Hydrometeor.*, **16**, 407–426, doi:10.1175/JHM-D-14-0105.1.

Lo Conti, F., K.-L. Hsu, L. V. Noto, and S. Sorooshian, 2014: Evaluation and comparison of satellite precipitation estimates with reference to a local area in the Mediterranean Sea. *Atmos. Res.*, **138**, 189–204, doi:10.1016/j.atmosres.2013.11.011.

Maggioni, V., R. H. Reichle, and E. N. Anagnostou, 2011: The effect of satellite rainfall error modeling on soil moisture prediction uncertainty. *J. Hydrometeor.*, **12**, 413–428, doi:10.1175/2011JHM1355.1.

——, H. J. Vergara, E. N. Anagnostou, J. J. Gourley, Y. Hong, and D. Stampoulis, 2013: Investigating the applicability of error correction ensembles of satellite rainfall products in river flow simulations. *J. Hydrometeor.*, **14**, 1194–1211, doi:10.1175/JHM-D-12-074.1.

——, M. R. P. Sapiano, R. F. Adler, Y. Tian, and G. J. Huffman, 2014: An error model for uncertainty quantification in high-time-resolution precipitation products. *J. Hydrometeor.*, **15**, 1274–1292, doi:10.1175/JHM-D-13-0112.1.

Mandapaka, P. V., W. F. Krajewski, R. Mantilla, and V. K. Gupta, 2009: Dissecting the effect of rainfall variability on the statistical structure of peak flows. *Adv. Water Resour.*, **32**, 1508–1525, doi:10.1016/j.advwatres.2009.07.005.

Mantilla, R., and V. K. Gupta, 2005: A GIS numerical framework to study the process basis of scaling statistics in river networks. *IEEE Geosci. Remote Sens. Lett.*, **2**, 404–408, doi:10.1109/LGRS.2005.853571.

Mehran, A., and A. AghaKouchak, 2014: Capabilities of satellite precipitation datasets to estimate heavy precipitation rates at different temporal accumulations. *Hydrol. Processes*, **28**, 2262–2270, doi:10.1002/hyp.9779.

Moazami, S., S. Golian, M. R. Kavianpour, and Y. Hong, 2014: Uncertainty analysis of bias from satellite rainfall estimates using copula method. *Atmos. Res.*, **137**, 145–166, doi:10.1016/j.atmosres.2013.08.016.

Nikolopoulos, E. I., E. N. Anagnostou, F. Hossain, M. Gebremichael, and M. Borga, 2010: Understanding the scale relationships of uncertainty propagation of satellite rainfall through a distributed hydrologic model. *J. Hydrometeor.*, **11**, 520–532, doi:10.1175/2009JHM1169.1.

——, ——, and M. Borga, 2013: Using high-resolution satellite rainfall products to simulate a major flash flood event in northern Italy. *J. Hydrometeor.*, **14**, 171–185, doi:10.1175/JHM-D-12-09.1.

Petersen, W. A., W. Krajewski, 2013: Status update on the GPM ground validation Iowa Flood Studies (IFloodS) field experiment. *Geophysical Research Abstracts*, Vol. 15, Abstract EGU2013-13345. [Available online at http://meetingorganizer.copernicus.org/EGU2013/EGU2013-13345.pdf.]

Qu, J. J., and A. M. Powell, 2013: Satellite-Based Applications on Climate Change. J. Qu, A. Powell, and M. V. K. Sivakumar, Eds., Springer, 371 pp.

Reed, S. M., and D. R. Maidment, 1999: Coordinate transformations for using NEXRAD data in GIS-based hydrologic modeling. *J. Hydrol. Eng.*, **4**, 174–182, doi:10.1061/(ASCE)1084-0699(1999)4:2(174).

Rodríguez-Iturbe, I., and A. Rinaldo, 2001: *Fractal River Basins: Chance and Self-Organization*. Rev. ed. Cambridge University Press, 570 pp.

Seo, B.-C., and W. F. Krajewski, 2010: Scale dependence of radar rainfall uncertainty: Initial evaluation of NEXRAD's new super-resolution data for hydrologic applications. *J. Hydrometeor.*, **11**, 1191–1198, doi:10.1175/2010JHM1265.1.

——, ——, and G. Villarini, 2012: Rain gauge data quality control and combining data from different networks for hydrologic applications. *2012 Fall Meeting*, San Francisco, CA, Amer. Geophys. Union, Abstract H41I-1278.

——, B. Dolan, W. F. Krajewski, S. A. Rutledge, and W. Petersen, 2015: Comparison of single and dual polarization based rainfall estimates using NEXRAD data for the NASA Iowa Flood Studies project. *J. Hydrometeor.*, **16**, 1658–1675, doi:10.1175/JHM-D-14-0169.1.

Serpetzoglou, E., E. N. Anagnostou, A. Papadopoulos, E. I. Nikolopoulos, and V. Maggioni, 2010: Error propagation of remote sensing rainfall estimates in soil moisture prediction from a land surface model. *J. Hydrometeor.*, **11**, 705–720, doi:10.1175/2009JHM1166.1.

Small, S. J., L. O. Jay, R. Mantilla, R. Curtu, L. K. Cunha, M. Fonley, and W. F. Krajewski, 2013: An asynchronous solver for systems of ODEs linked by a directed tree structure. *Adv. Water Resour.*, **53**, 23–32, doi:10.1016/j.advwatres.2012.10.011.

Stampoulis, D., and E. N. Anagnostou, 2012: Evaluation of global satellite rainfall products over continental Europe. *J. Hydrometeor.*, **13**, 588–603, doi:10.1175/JHM-D-11-086.1.

——, ——, and E. I. Nikolopoulos, 2013: Assessment of high-resolution satellite-based rainfall estimates over the Mediterranean during heavy precipitation events. *J. Hydrometeor.*, **14**, 1500–1514, doi:10.1175/JHM-D-12-0167.1.

Thiemig, V., R. Rojas, M. Zambrano-Bigiarini, and A. De Roo, 2013: Hydrological evaluation of satellite-based rainfall estimates over the Volta and Baro-Akobo basin. *J. Hydrol.*, **499**, 324–338, doi:10.1016/j.jhydrol.2013.07.012.

Tong, K., F. Su, D. Yang, and Z. Hao, 2014: Evaluation of satellite precipitation retrievals and their potential utilities in hydrologic modeling over the Tibetan Plateau. *J. Hydrol.*, **519**, 423–437, doi:10.1016/j.jhydrol.2014.07.044.

Vergara, H., Y. Hong, J. J. Gourley, E. N. Anagnostou, V. Maggioni, D. Stampoulis, and P.-E. Kirstetter, 2014: Effects of resolution of satellite-based rainfall estimates on hydrologic modeling skill at different scales. *J. Hydrometeor.*, **15**, 593–613, doi:10.1175/JHM-D-12-0113.1.

Villarini, G., and W. F. Krajewski, 2007: Evaluation of the research version TMPA three-hourly 0.25° × 0.25° rainfall estimates over Oklahoma. *Geophys. Res. Lett.*, **34**, L05402, doi:10.1029/2006GL029147.

——, and ——, 2010: Review of the different sources of uncertainty in single polarization radar-based estimates of rainfall. *Surv. Geophys.*, **31**, 107–129, doi:10.1007/s10712-009-9079-x.

Worqlul, A. W., A. S. Collick, S. A. Tilahun, S. Langan, T. H. M. Rientjes, and T. S. Steenhuis, 2015: Comparing TRMM 3B42, CFSR and ground-based rainfall estimates as input for hydrological models, in data scarce regions: The Upper Blue Nile basin, Ethiopia. *Hydrol. Earth Syst. Sci. Discuss.*, **12**, 2081–2112, doi:10.5194/hessd-12-2081-2015.

Wu, H., R. F. Adler, Y. Hong, Y. Tian, and F. Policelli, 2012: Evaluation of global flood detection using satellite-based rainfall and a hydrologic model. *J. Hydrometeor.*, **13**, 1268–1284, doi:10.1175/JHM-D-11-087.1.

——, ——, Y. Tian, G. J. Huffman, H. Li, and J. Wang, 2014: Real-time global flood estimation using satellite-based precipitation and a coupled land surface and routing model. *Water Resour. Res.*, **50**, 2693–2717, doi:10.1002/2013WR014710.

Young, M. P., C. J. R. Williams, J. C. Chiu, R. I. Maidment, and S.-H. Chen, 2014: Investigation of discrepancies in satellite rainfall estimates over Ethiopia. *J. Hydrometeor.*, **15**, 2347–2369, doi:10.1175/JHM-D-13-0111.1.

Zhao, H., S. Yang, Z. Wang, X. Zhou, Y. Luo, and L. Wu, 2015: Evaluating the suitability of TRMM satellite rainfall data for hydrological simulation using a distributed hydrological model in the Weihe River catchment in China. *J. Geogr. Sci.*, **25**, 177–195, doi:10.1007/s11442-015-1161-3.